

Electrochemical corrosion of Sn–0.75Cu solder joints in NaCl solution

GAO Yan-fang¹, CHENG Cong-qian¹, ZHAO Jie¹, WANG Li-hua¹, LI Xiao-gang²

1. School of Materials Science and Engineering, Dalian University of Technology, Dalian 116085, China;

2. School of Materials Science and Engineering, Beijing University of Science and Technology,
Beijing 100083, China

Received 26 April 2011; accepted 14 October 2011

Abstract: The corrosion behaviors of Sn–0.75Cu solder and Sn–0.75Cu/Cu joint in 3.5% NaCl (mass fraction) solution were studied by potentiodynamic polarization test and leaching measurement. The polarization curves indicated that the corrosion rate of Sn–0.75Cu solder was lower than that of Sn–0.75Cu/Cu joint. The morphology observation and phase composition analysis on the corroded product at each interesting potential suggested that $\text{Sn}_3\text{O}(\text{OH})_2\text{Cl}_2$ formed on the surface of Sn–0.75Cu solder at active dissolution stage. As the potential increased from active/passive transition stage, all the surface of Sn–0.75Cu solder was covered by the $\text{Sn}_3\text{O}(\text{OH})_2\text{Cl}_2$ and some pits appeared after the polarization test. Compared to the Sn–0.75Cu solder alloy, much more $\text{Sn}_3\text{O}(\text{OH})_2\text{Cl}_2$ formed at active dissolution stage and the pits with bigger size were observed after polarization test for the Sn–0.75Cu/Cu solder joints. The leaching test confirmed that the faster electrochemical corrosion rate resulted in the larger amount of Sn released from the Sn–0.75Cu/Cu solder joints.

Key words: Sn–0.75Cu solder; Sn–0.75Cu/Cu joint; corrosion; potentiodynamic polarization; leaching behavior; corroded products

1 Introduction

Nowadays, to develop lead-free solders to replace lead-bearing solders, many progresses have been achieved in Sn–Ag, Sn–Zn, and Sn–Cu solder alloys [1–3]. Although the replacement of Pb-bearing solders by several favorable solder alloys can avoid potential environmental risk from toxic Pb elements, excessive of other elements, such as Ag, Cu, and Zn, released into the environment due to corrosion would still pose a concern to ecosystems and human health [4,5]. It is therefore essential to evaluate the corrosion property of newly developed lead-free solders.

Several studies have been carried out to examine the corrosion behavior of lead-free solder alloys [6–9]. As for achieving higher circuit board component densities, package dimensions have been shrinking with decreasing solder bump sizes, and thus the area ratio of solder alloys to substrates is becoming small. Spontaneously, the effect of substrates on the corrosion property of solders can not be ignored. For example, the corrosion property of Sn–Ag–Cu, Sn–Ag–Cu–Bi and Sn–Pb solder joints

in deionized water was researched by CHANG et al [10] and they obtained that the substrate as cathode could lead to the formation of SnO crystals on the solder surface, and the corrosion rate of solders increased with the increase of cathode area. LIU et al [11] studied the electrochemical corrosion property of Sn–9Zn–1.5Ag–1Bi alloy/Cu joint in 3.5% NaCl solution and found that some pits formed at solder/substrate interfaces. In our previous work [12,13], the corrosion property of several solders and their joints had been studied by leaching test. It was found that the leaching amount of Sn from the solder joints was much larger than that from the corresponding solder alloys, which might be attributed to the accelerating electrochemical corrosion caused by Cu substrate. Unfortunately, few literatures have reported on the difference of electrochemical corrosion mechanism between the solder alloys and their joints. Moreover, up to now, the relationship between the leaching and electrochemical corrosion has not been realized.

Although Sn–Cu solder alloy is one of the most promising solders in electronic packaging owing to its low cost and good comprehensive properties among many alternative lead-free solder alloys [14,15], the

corrosion behavior of Sn–Cu solder alloy and its joints has not been extensively researched. In the present work, the corrosion property of Sn–0.75Cu solder and Sn–0.75Cu/Cu joint in 3.5% NaCl solution was investigated by potentiodynamic polarization and leaching test. In particular, the microstructure and composition of corroded products during each polarization were examined to understand the corrosion procedure of Sn–0.75Cu solder and Sn–0.75Cu/Cu joint.

2 Experimental

Sn–0.75Cu solder alloy in the current work was prepared from pure Sn and Cu metals with a purity of 99.99%. The Sn and Cu metals were degreased with 5% NaOH solution, deoxidized with 5% HCl (volume fraction), and rinsed with deionized water. And then they were weighed and melted at 600 °C in a vacuum furnace in the protection of nitrogen atmosphere. The Sn–0.75Cu alloy and Cu substrates were cut into samples with size of dimensions of 7 mm×8 mm×1 mm and ground with sandpapers down to 2500 grid. Subsequently, the Sn–0.75Cu/Cu solder joints were obtained by diffusion bonding in a vacuum furnace at 200 °C for 20 h.

The potentiodynamic polarization tests were carried out in 3.5% NaCl solution at temperature of (45±3) °C. Prior to each measurement, the samples were ground with sandpapers to 2000 grid and rinsed with distilled water to expose a fresh surface. The exposed solder area was about 56 mm². For Sn–0.75Cu/Cu joint, the working area consisted of 56 mm² solder and the same area of Cu plate. Before testing, oxygen was injected into the freshly prepared solution with the volume of 300 mL by a gas flowmeter at a flow rate of 45 mL/min for 10 min. The test cell consisted of the sample as a working electrode, a platinum foil as a counter electrode and a saturated calomel electrode (SCE) as a reference electrode with a Luggin capillary bridge connected to the test solution. Before polarization scanning, the specimens were cathodically treated in the electrolyte until the open potential was stable and then tested from –200 to 1600 mV (vs SCE) of the open potential at a scan rate of 1 mV/s. The surface morphology of samples polarized to different potential was observed by scanning electron microscopy (SEM, JSM5600-LV) and analyzed by energy dispersive X-ray spectroscopy (EDX). The phase of the corrosion products was identified by X-ray diffraction (XRD, Bruker D8 Focus) using Cu K_α radiation, operating at 40 kV, 40 mA and a scanning rate of 4(°)/min for 2θ from 20° to 100°.

The method of the leaching experiments for Sn–075Cu solder alloy and Sn–075Cu/Cu joint was the same as that described in our previous work [13], and the testing periods were 15, 30 and 45 d in this work. For

each period of the leaching test, three samples were measured and the results were averaged to ensure the reliability of the results. The variance of the results (calculated by root mean square deviation) was expressed by the error bars in the graph.

3 Results and discussion

3.1 Electrochemical corrosion of Sn–0.75Cu solder, Sn–0.75Cu/Cu joint and Cu substrate

The polarization curves of Sn–0.75Cu solder, Sn–0.75Cu/Cu joint and Cu in 3.5% NaCl solution are illustrated in Fig. 1 and the data from these curves are listed in Table 1. Sn–0.75Cu solder alloy and Sn–0.75Cu/Cu joint were denoted by SC and SC*, respectively. And the detailed analysis was carried out at different points (A–F) in polarization curves later.

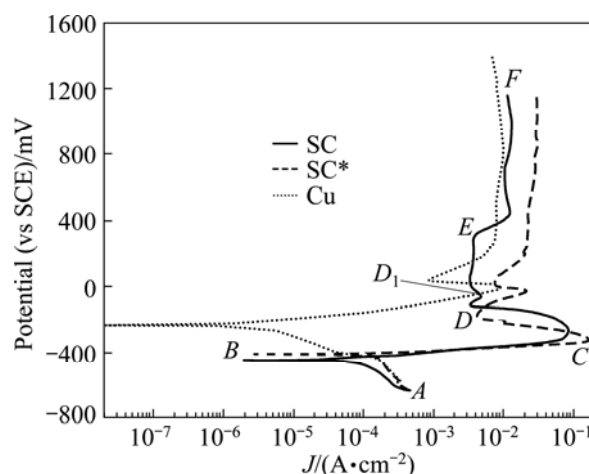


Fig. 1 Polarization curves of Sn-0.75Cu(SC), Sn-0.75Cu/Cu(SC*) and Cu in 3.5% NaCl solution

Table 1 Electrochemical properties of samples in 3.5% NaCl solution

Material	$\varphi_{\text{corr}}/$ mV	$J_{\text{corr}}/$ (A·cm ⁻²)	$\varphi_{\text{pp}}/$ mV	$J_{\text{cc}}/$ (A·cm ⁻²)	$\varphi_{\text{bd}}/$ mV	$J_{\text{p}}/$ (A/cm ⁻²)
SC	-446	9.51×10^{-5}	-269	8.153×10^{-2}	289	3.73×10^{-3}
SC*	-409	1.74×10^{-4}	-323	0.162	32	7.80×10^{-3}
Cu	-232	4.64×10^{-6}	-8	8.69×10^{-3}	–	–

3.1.1 Reaction on cathode

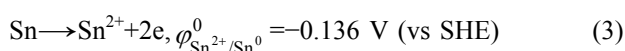
The corrosion tests were performed in NaCl solution with saturated oxygen at the beginning of testing, and the initial reactions occurring on the cathode (stage AB) were the dissolved oxygen reduction reaction (1) and hydrogen evolution reaction (2).



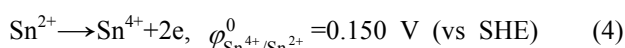
The first reaction dominated until the dissolved oxygen in the solution was completely consumed. Then some hydrogen bubbles caused by the hydrogen evolution began to gather on the cathode and the reaction (2) became the main step.

3.1.2 Active dissolution of anode

The current density increased rapidly from point *B* where active Sn dissolved into Sn^{2+} according to the following reaction [16]:



where $\varphi_{\text{Sn}^{2+}/\text{Sn}^0}^0$ is the standard oxidation potential. And Sn^{2+} further oxidized to Sn^{4+} according to



The potential at point *B* was named as the corrosion potential (φ_{corr}). The corrosion current density J_{corr} which represented the corrosion rate of the system was determined by Tafel extrapolation. From Fig. 1 and Table 1, it can be known that φ_{corr} value of Sn–0.75Cu solder is similar to that of Sn–0.75Cu/Cu joint, but much lower than that of Cu substrate. The corrosion current density of Sn–0.75Cu solder alloy is $9.51 \times 10^{-5} \text{ A/cm}^2$, lower than that of Sn–0.75Cu/Cu ($1.74 \times 10^{-4} \text{ A/cm}^2$), which indicates a higher corrosion rate in the joint. During the polarization tests of joints, black products formed on the surface of Sn–0.75Cu but no product was observed on the Cu plate surface. This result suggested that the corrosion reaction only occurred on the surface of the Sn–0.75Cu with inferior corrosion resistance than Cu plate.

The active dissolution of Sn continued with the increase of current density till the current density reached a maximum at point *C*. The potential and current density at point *C* were referred as the passivation potential (φ_{pp}) and critical current density (J_{cc}), respectively. It is noted from Table 1 that the Sn–0.75Cu/Cu joint has the lowest φ_{pp} and the highest J_{cc} , which suggests that Cu increases the passivation capability of Sn–0.75Cu but decreases the protection performance of the initial passive film. The corroded surface morphologies of SC and SC* are shown in Figs. 2 and 3. The XRD patterns of corroded product on the solder surface are shown in Fig. 4. For Sn–0.75Cu solder alloy, small amount of corroded products formed on the surface of solder alloy, as pointed out in Fig. 2(a), while most surface of Sn–0.75Cu/Cu joints was covered by corroded product, as shown in Fig. 2(b). The EDX results suggested that all the products of the samples were oxides containing Sn, Cl, and O. Figure 4(a) shows the XRD patterns of corroded products on the solder surface when the specimen polarized to point *C*. And it can be identified that the corroded product was $\text{Sn}_3\text{O}(\text{OH})_2\text{Cl}_2$, which might be formed through the following reaction [17]:



The same product was reported by YU et al [18] when they studied the corrosion behavior of Sn–9Zn and Sn–8Zn–3Bi in the NaCl solution. MOHANTY and LIN [19] also suggested that SnCl_2 could absorb O_2 to form insoluble oxychloride. Our experimental result was well consistent with the previous researches.

3.1.3 Active/passive transition stage

The current slowly decreased from point *C* and it was almost independent of potential at point *D*. And the region of *CD* was regarded as active/passive transition stage. Figs. 2(c) and (d) illustrated the surface morphology of Sn–0.75Cu solder and Sn–0.75Cu/Cu joint when the samples polarized up to point *D*. It revealed that products with needle-like and sheet-like structures were loosely distributed on the surface. Moreover, some pores were observed on the Sn–0.75Cu surface and the amount of pores in the joint is larger than that in the solder alloy. The XRD result of the samples that polarized to point *D*, as shown in Fig. 4(b), suggested that both needle-like and sheet-like products were $\text{Sn}_3\text{O}(\text{OH})_2\text{Cl}_2$. The structure of $\text{Sn}_3\text{O}(\text{OH})_2\text{Cl}_2$ was similar to that reported by CHANG et al [20] for Sn–3.5Ag alloy.

3.1.4 Stable passivation stage

The corrosion was blocked by the stable passive film and the current density dropped to a low value (J_{p}) at point *D*. For Sn–0.75Cu solder, a small current peak D_1 formed close to the passivation peak *D*, as shown in Fig. 1. And this might be attributed to the competition between the formation and chemical dissolution of the passive film [21]. However, from point D_1 , the solder alloy exhibited a passivation current density (J_{p}) of $3.73 \times 10^{-3} \text{ A/cm}^2$ while the passivation range extended from 2 to 291 mV (vs SCE). In contrast, the J_{p} value of Sn–0.75Cu/Cu joint was $7.87 \times 10^{-3} \text{ A/cm}^2$ when the passivation range extended from –14 to +32 mV (vs SCE). The larger passivation range and lower passivation current density illustrated that the passive film on Sn–0.75Cu solder alloy is more stable and protective than on Sn–0.75Cu/Cu joint [22]. The SEM micrographs of the corroded products on the surface of Sn–0.75Cu solder and Sn–0.75Cu/Cu joint when they polarized to point *E* are shown in Figs. 3(a) and (b), respectively. It was found that the Sn–0.75Cu surface was completely covered by the needle-like and sheet-like corroded products with compact microstructures. The XRD pattern of the solder when it polarized to point *E* is shown in Fig. 4(c), which denotes that the product is $\text{Sn}_3\text{O}(\text{OH})_2\text{Cl}_2$.

3.1.5 Breakdown of passive film

From point *E*, a large increase in the current density

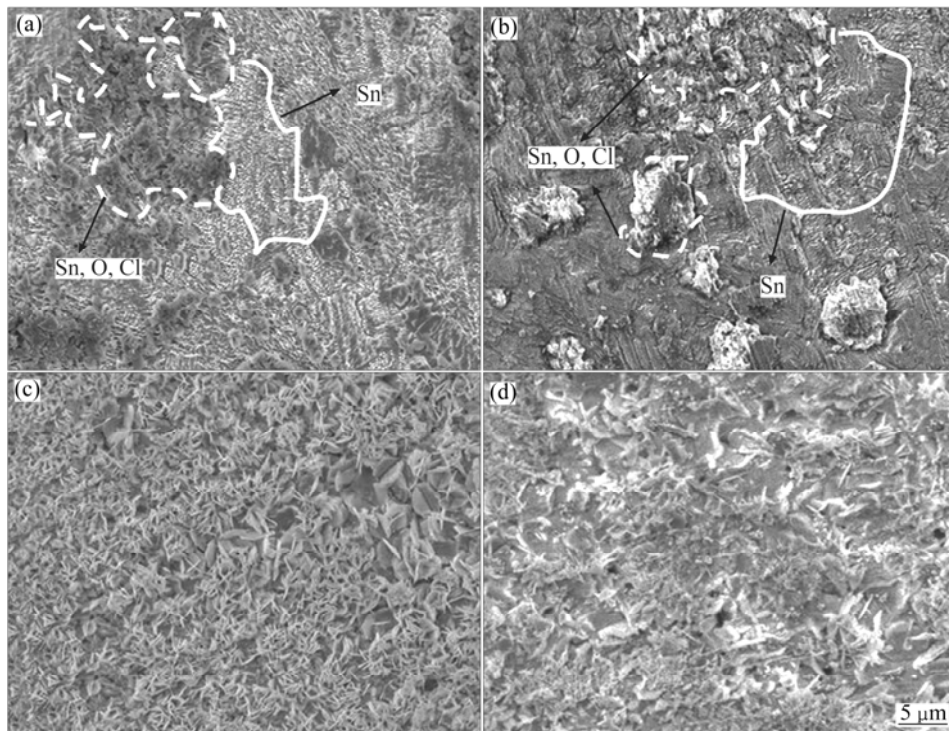


Fig. 2 Micrographs of corroded surface of SC and SC* polarized to points *C* and *D*: (a) SC at point *C*; (b) SC* at point *C*; (c) SC at point *D*; (d) SC* at point *D*

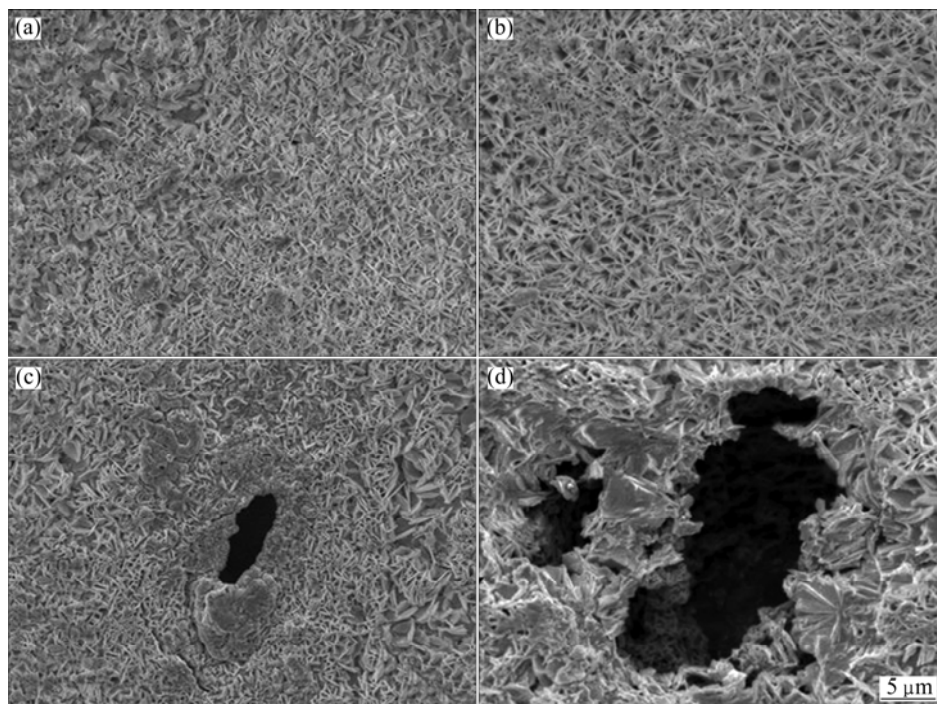


Fig. 3 Micrographs of corroded surface of SC and SC* polarized to point *E* and *F*: (a) SC at point *E*; (b) SC* at point *E*; (c) SC at point *F*; (d) SC* at point *F*

accompanied with a small increase in the anodic potential indicates the breakdown of the passive film. In the surface morphology of Sn–0.75Cu solder alloy and Sn–0.75Cu/Cu joint after electrochemical tests shown in Figs. 3(c) and (d), some deep pits were found. And the

size of pits on the surface of Sn–0.75Cu joint is larger than that on solder alloy surface. COTTON and WILKINSON [23] and REFAEY [24] considered the active dissolution of Sn stimulated by the aggressive Cl^- ion with the formation of soluble complexes was the

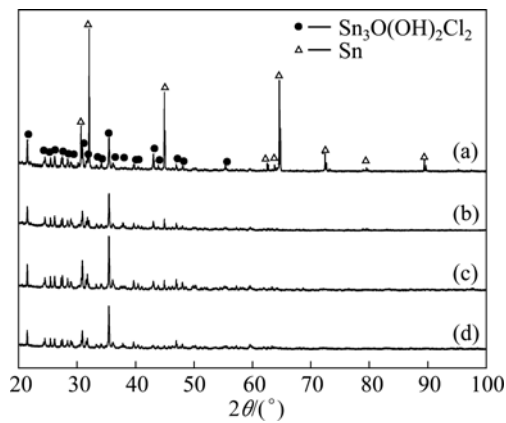


Fig. 4 XRD patterns of surface product on SC surface when SC polarized to different point: (a) SC at point C; (b) SC at point D; (c) SC at point E; (d) SC at point F

reason of the appearance of pits. It was reported by CHANG et al [20] that the corroded products near the pits for Sn–Zn–Ag alloy were composed of SnCl_2 , SnO and ZnO . LIN and LIU [25] also found that the corroded products on the surface might be SnO , SnO_2 , SnCl_4 and ZnCl_2 , etc for Al–Zn–Sn in NaCl solution. However, only $\text{Sn}_3\text{O}(\text{OH})_2\text{Cl}_2$ product was observed in the current research, and the products containing Sn^{4+} species were not observed. The difference of corroded products in the polarization test might be largely depended on the composition of solder alloys and corrosive media.

3.2 Relationship between leaching and electrochemical behavior

The amounts of Sn leached from Sn–0.75Cu alloy and Sn–0.75Cu/Cu joint in 3.5% NaCl solution after 15, 30 and 45 d immersion are shown in Fig. 5. During the testing period, there was no obvious change in the leaching amount of Sn from solder alloys; however, the leaching amount of Sn from Sn–0.75Cu/Cu joints increased rapidly with the increase of immersion time. The research on the corrosion behavior of joints in deionized water suggests that the substrate could accelerate the corrosion reaction of solder alloys due to the different potential ($\phi_{\text{Cu}^{2+}/\text{Cu}}^0 = 0.345$ and $\phi_{\text{Sn}^{2+}/\text{Sn}}^0 = -0.136$ V (vs SHE) [10]. And in the present study, the corrosion potentials of Sn–0.75Cu solder and Cu plate were -409 and -232 mV (vs SCE), respectively. Consequently, a large amount of Sn was leached from Sn–0.75Cu/Cu joint. The corrosion property research out of Sn alloys by dipping tests was by MORI et al [6] who reported that the electrochemical reaction of Sn was the reason for the dissolution of Sn. Therefore, the comparison between leaching behavior and electrochemical results of Sn–0.75Cu solder and Sn–0.75Cu/Cu joint was carried.

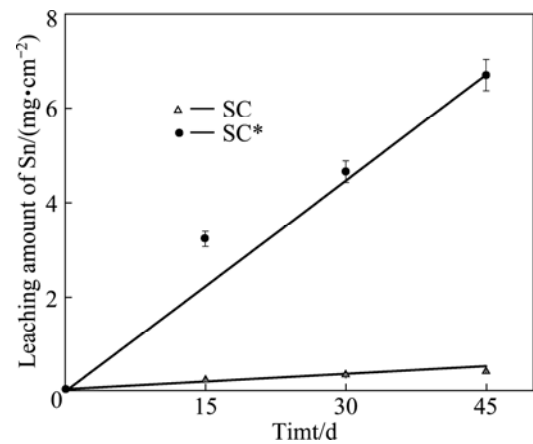


Fig. 5 Leaching amount of Sn from SC and SC* after being immersed in 3.5% NaCl solution

The slope of leaching amount of Sn varying with time obtained from Fig. 5 can present the leaching rate of Sn–0.75Cu solder alloys and Sn–0.75Cu/Cu joint. Meanwhile, according to Faraday's law, the J_{corr} obtained by Tafel method can be converted to the corrosion rate in unit of mm/a, if the valency of the metallic ion is known. The comparison between the current density and the leaching rate of Sn is shown in Fig. 6. It is noted from Fig. 6 that the joint has a higher J_{corr} value and leaching rate for Sn–0.75Cu/Cu joint while a lower J_{corr} value and leaching rate for the Sn–0.75Cu solder. Thus, the results of leaching experiment are in accordance with the electrochemical polarization tests.

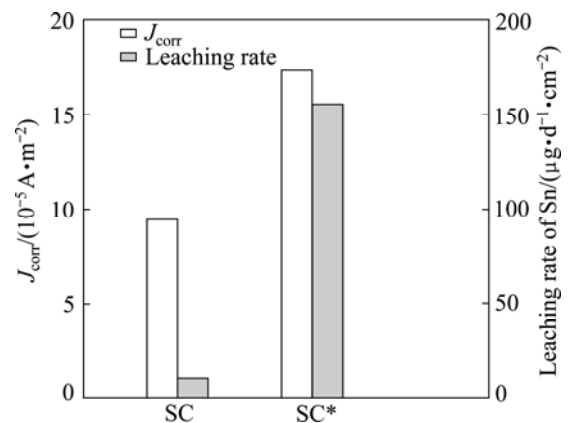


Fig. 6 Relationship between leaching rate of Sn and corrosion current density

4 Conclusions

- 1) The potentiodynamic polarization tests suggested that the corrosion rate of Sn–0.7Cu/Cu joint is higher than that of Sn–0.75Cu solder alloy in 3.5% NaCl solution.
- 2) The corroded product on the surface of the solder and the joint is a small amount of $\text{Sn}_3\text{O}(\text{OH})_2\text{Cl}_2$ at active

dissolution stage. And from the active/passive transition, the surface is completely covered by $\text{Sn}_3\text{O}(\text{OH})_2\text{Cl}_2$. Besides, some pits formed on the Sn–0.75Cu surface of the both solder and joint, and the pits on the joint are bigger than that those on the solder alloy.

3) The leaching amount of Sn from Sn–0.7Cu solder alloys is much lower than that from Sn–0.7Cu/Cu joint in each testing period. And the results are consistent with that obtained by corrosion current density of polarization tests.

References

- [1] WU C M L, YU D Q, LAW C M T, WANG L. Properties of lead-free solder alloys with rare earth element additions [J]. Mater Sci Eng R, 2004, 44: 1–44.
- [2] ZENG K, TU K N. Six cases of reliability study of Pb-free solder joints in electronic packaging technology [J]. Mater Sci Eng R, 2002, 38: 55–105.
- [3] ABTEW M, SELVADURAY G. Lead-free solders in microelectronics [J]. Mater Sci Eng R, 2000, 27: 95–141.
- [4] WILMOTH R C, HUBBARD S, BURCKLE J O, MARTIN J F. Production and processing of metals: Their disposal and future risks [C]//MERIAN E. Metals and their compounds in the environment: occurrence, analysis and biological relevance. Berlin: Wiley-VCH, Weinheim, 1991: 19–65.
- [5] LIM S R, SCHOENUNG J M. Human health and ecological toxicity potentials due to heavy metal content in waste electronic devices with flat panel displays [J]. J Hazard Mater, 2010, 177: 251–259.
- [6] MORI M, MIURA K, SASAKI T, OHTSUKA T. Corrosion of tin alloys in sulfuric and nitric acids [J]. Corros Sci, 2002, 44: 887–898.
- [7] MOHANTY U S, LIN K L. The polarization characteristics of Pb-free Sn–8.5Zn–xAg–0.1Al–0.05Ga alloy in 3.5% NaCl solution [J]. Corros Sci, 2007, 49: 2815–2831.
- [8] MOHANTY U S, LIN K L. Electrochemical corrosion behaviour of Pb-free Sn–8.5Zn–0.05Al–xGa and Sn–3Ag–0.5Cu alloys in chloride containing aqueous solution [J]. Corros Sci, 2008, 50: 2437–2443.
- [9] ROSALBINO F, ANGELINI E, ZANICCHI G, MARAZZA R. Corrosion behaviour assessment of lead-free Sn–Ag–M (M=In, Bi, Cu) solder alloys [J]. Mater Chem Phys, 2008, 109: 386–391.
- [10] CHANG H, CHEN H T, LI M Y, WANG L, FU Y G. Generation of tin (II) oxide crystals on lead-free solder joints in deionized water [J]. J Electron Mater, 2009, 38(10): 2170–2178.
- [11] LIU C Y, CHEN Y R, LI W L, HON M H, WANG M C. Electrochemical properties of joints formed between Sn–9Zn–1.5Ag–1Bi alloys and Cu substrates in a 3.5 wt.% NaCl solution [J]. J Electron Mater, 2007, 36: 1532–1535.
- [12] ZHAO Jie, MENG Xian-ming, CHEN Chen, ZANG Hua-xun, MA Hai-tao. Leaching behavior of heavy metal elements in lead-free solders [J]. J Environ Sci, 2008, 29(8): 2341–2344. (in Chinese)
- [13] CHENG C Q, YANG F, ZHAO J, WANG L H, LI X G. Leaching behavior of heavy metal elements in solder alloys [J]. Corros Sci, 2011, 53: 1738–1747.
- [14] WANG H Q, WANG F J, GAO F, MA X, QIAN Y Y. Reactive wetting of Sn0.7Cu–xZn lead-free solders on Cu substrate [J]. J Alloys Compd, 2007, 433: 302–305.
- [15] SURASKI D, SEELIG K. The current status of lead-free solder alloys [J]. IEEE Trans Electron Packag Manage, 2001, 23: 244–248.
- [16] MOHRAN S H, EL-SAYED A R, EL-LATEEF H M A. Anodic behavior of tin, indium, and tin-indium alloys in oxalic acid solution [J]. J Solid State Electrochem, 2009, 13: 1279–1290.
- [17] LI D Z, CONWAY P, LIU C Q. Corrosion characterization of tin-lead and lead in 3.5wt.% NaCl solution [J]. Corros Sci, 2008, 50: 995–1004.
- [18] YU Da-quan, WU C M L, WANG Lai. The electrochemical corrosion behavior of Sn–9Zn and Sn–8Zn–3Bi lead-free solder alloys in NaCl solution [C]//16th International Corrosion Congress. Beijing, China, 2005:19–24.
- [19] MOHANTY U S, LIN K L. Electrochemical corrosion behaviour of lead-free Sn–8.5Zn–xAg–0.1Al–0.5Ga solder in 3.5% NaCl solution [J]. Mater Sci Eng A, 2005, 406: 34–42.
- [20] CHANG T C, HON M H, WANG M C, LIN D Y. Electrochemical behaviors of the Sn–9Zn–xAg lead-free solders in a 3.5 wt % NaCl solution [J]. J Electrochem Soc, 2004, 151(7): C484–C491.
- [21] ZHU X L, SANDENBERGH R F. Corrosion of tinplate T54S and T61 in humid atmosphere and saline solution [J]. Mater Corros, 2001, 52: 685–690.
- [22] SINGH V B, GUPTA A. Active, passive and transpassive dissolution of In-718 alloy in acidic solutions [J]. Mater Chem Phys, 2004, 85: 12–19.
- [23] COTTON F A, WILKINSON G. Advanced inorganic chemistry [M]. 3rd ed. New York: Interscience Publishers, 1972: 330.
- [24] REFAEY S A M. The corrosion and passivation of tin in borate solutions and the effect of halide [J]. Electrochim Acta, 1996, 41: 2545–2549.
- [25] LIN K L, LIU T P. The electrochemical corrosion behavior of Pb-free Al–Zn–Sn solders in NaCl solution [J]. Mater Chem Phys, 1998, 56: 171–176.

Sn–0.75Cu 钎料接头在 NaCl 溶液中的电化学腐蚀行为

高艳芳¹, 程从前¹, 赵杰¹, 王丽华¹, 李晓刚²

1. 大连理工大学 材料科学与工程学院, 大连 116085; 2. 北京科技大学 材料科学与工程学院, 北京 100083

摘要: 采用动电位极化及浸出方法研究 Sn–0.75Cu 钎料及 Sn–0.75Cu/Cu 接头在 3.5% NaCl 溶液中的电化学腐蚀行为。极化曲线测试结果表明 Sn–0.75Cu 钎料的腐蚀速率比 Sn–0.75Cu/Cu 接头的低。在特殊电位时的形貌观察及相分析表明, 在 Sn–0.75Cu 钎料表面活化溶解区形成腐蚀产物 $\text{Sn}_3\text{O}(\text{OH})_2\text{Cl}_2$ 。从活化/钝化区开始, Sn–0.75Cu 钎料的表面完全被腐蚀产物 $\text{Sn}_3\text{O}(\text{OH})_2\text{Cl}_2$ 覆盖, 并且在极化测试后出现蚀坑。与 Sn–0.75Cu 钎料合金相比, Sn–0.75Cu/Cu 接头的钎料表面在活化区形成较多的 $\text{Sn}_3\text{O}(\text{OH})_2\text{Cl}_2$, 在极化测试结束时腐蚀坑的尺寸较大。浸出实验结果证实了 Sn–0.75Cu/Cu 接头较快的电化学腐蚀速率引起较多的 Sn 从中接头中释放出来。

关键词: Sn–0.75Cu 钎料; Sn–0.75Cu/Cu 接头; 腐蚀; 动电位极化; 浸出行为; 腐蚀产物

(Edited by YANG Hua)